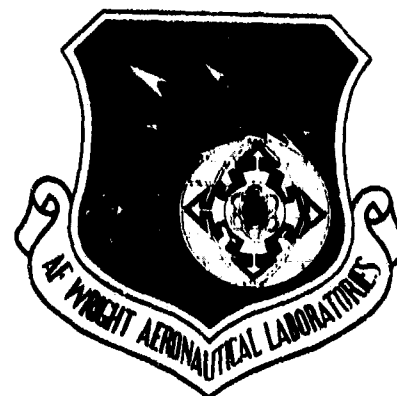


2

AFWAL-TR-84-3045



# USE OF QUATERNIONS IN FLIGHT MECHANICS

WILBUR L. HANKEY  
L. EARL MILLER  
STEPHEN J. SCHERR

Aerodynamics and Airframe Branch (AFWAL/FIMM)  
High Speed Aero Performance Branch (AFWAL/FIMG)  
Aeromechanics Division (AFWAL/FIM)

March 1984

Final Technical Report

Approved for public release; distribution unlimited

FLIGHT DYNAMICS LABORATORY  
AIR FORCE WRIGHT AERONAUTICAL LABORATORIES  
AIR FORCE SYSTEMS COMMAND  
WRIGHT-PATTERSON AIR FORCE BASE, OHIO 45433

DTIC  
ELECTE  
APR 22 1985  
S E D

85 03 28 055

AD-A152 616


DTIC FILE COPY

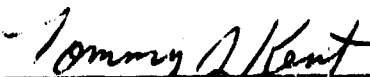
# NOTICE

When Government drawings, specifications, or other data are used for any purpose other than in connection with a definitely related Government procurement operation, the United States Government thereby incurs no responsibility nor any obligation whatsoever; and the fact that the government may have formulated, furnished, or in any way supplied the said drawings, specifications, or other data, is not to be regarded by implication or otherwise as in any manner licensing the holder or any other person or corporation, or conveying any rights or permission to manufacture use, or sell any patented invention that may in any way be related thereto.


This report has been reviewed by the Office of Public Affairs (ASD/PA) and is releasable to the National Technical Information Service (NTIS). At NTIS, it will be available to the general public, including foreign nations.

This technical report has been reviewed and is approved for publication.

  
JOSEPH S. SHANG  
Project Engineer

  
TOMMY J. KENT, Maj, USAF  
Chief, Aerodynamics & Airframe Branch  
Aeromechanics Division

FOR THE COMMANDER

  
RALPH W. HOLM, Col, USAF  
Chief, Aeromechanics Division

"If your address has changed, if you wish to be removed from our mailing list, or if the addressee is no longer employed by your organization please notify AFWAL/FIMM, W-PAFB, OH 45433 to help us maintain a current mailing list".

Copies of this report should not be returned unless return is required by security considerations, contractual obligations, or notice on a specific document.

UNCLASSIFIED

SECURITY CLASSIFICATION OF THIS PAGE

AD-A152616

## REPORT DOCUMENTATION PAGE

1a. REPORT SECURITY CLASSIFICATION <b>UNCLASSIFIED</b>		1b. RESTRICTIVE MARKINGS	
2a. SECURITY CLASSIFICATION AUTHORITY		3. DISTRIBUTION/AVAILABILITY OF REPORT  Distribution Unlimited	
2b. DECLASSIFICATION/DOWNGRADING SCHEDULE		5. MONITORING ORGANIZATION REPORT NUMBER(S)	
4. PERFORMING ORGANIZATION REPORT NUMBER(S)  AFWAL-TR-84-3045		7a. NAME OF MONITORING ORGANIZATION	
6a. NAME OF PERFORMING ORGANIZATION Flight Dynamics Laboratory AFWAL/FIMM	6b. OFFICE SYMBOL (If applicable) AFWAL/FIMM	7b. ADDRESS (City, State and ZIP Code)	
6c. ADDRESS (City, State and ZIP Code) Flight Dynamics Laboratory (AFWAL/FIMM) AF Wright Aeronautical Laboratories (AFSC) Wright-Patterson Air Force Base, OH 45433		9. PROCUREMENT INSTRUMENT IDENTIFICATION NUMBER	
8a. NAME OF FUNDING/SPONSORING ORGANIZATION	8b. OFFICE SYMBOL (If applicable)	10. SOURCE OF FUNDING NOS.	
8c. ADDRESS (City, State and ZIP Code)		PROGRAM ELEMENT NO.	PROJECT NO. 2307
11. TITLE (Include Security Classification) <b>UNCLASSIFIED</b> USE OF QUATERNIONS IN FLIGHT MECHANICS		TASK NO. N6	WORK UNIT NO. 03
12. PERSONAL AUTHOR(S) Wilbur L. Hankey, L. Earl Miller, Stephen J. Scherr			
13a. TYPE OF REPORT Final Technical Report	13b. TIME COVERED FROM Jul 82 TO Sep 83	14. DATE OF REPORT (Yr., Mo., Day) 1984 March	15. PAGE COUNT 48
16. SUPPLEMENTARY NOTATION			
17. COSATI CODES		18. SUBJECT TERMS (Continue on reverse if necessary and identify by block number)	
FIELD	GROUP	SUB. GR.	
01	01		
19. ABSTRACT (Continue on reverse if necessary and identify by block number)			
<p>Classical flight mechanics employ velocity coordinate or body axes systems. The latter uses Euler angles to define the aircraft orientation. Singularities and ambiguities occur whenever the flight path or elevation angle is plus or minus ninety degrees. These problems are circumvented through the use of quaternions. Two problems are addressed; the first is a nonsymmetric body and the second is a symmetrical configuration. The rotational dynamics and the solution for the quaternions and Euler angles are determined for both problems.</p>			
20. DISTRIBUTION/AVAILABILITY OF ABSTRACT  UNCLASSIFIED/UNLIMITED <input checked="" type="checkbox"/> SAME AS RPT. <input type="checkbox"/> DTIC USERS <input type="checkbox"/>		21. ABSTRACT SECURITY CLASSIFICATION  UNCLASSIFIED	
22a. NAME OF RESPONSIBLE INDIVIDUAL  Wilbur L. Hankey		22b. TELEPHONE NUMBER (Include Area Code) (513) 255-2455	22c. OFFICE SYMBOL  AFWAL/FIMM

## FOREWORD

This report was prepared by personnel of the Flight Mechanics Division of the Flight Dynamics Laboratory, Wright Aeronautical Laboratories (AFWAL/FIM), Wright-Patterson Air Force Base, Ohio. This research was accomplished under Task 2307N603, "Computational Aerodynamics".

The effort reported here covered the period July 1982 to September 1983. Dr. Wilbur Hankey and Steve Scherr (FIMM) accomplished the original work. Dr. Earl Miller (FIMG) starting in June 1983, revised and extended the results of Technical Memorandum AFWAL-TM-83-178, "Use of Quaternion to Numerically Analyze Aircraft Spin". This TM was used as the basis for this technical report.

Accession For	
NTIS GRA&I	<input checked="checked" type="checkbox"/>
DTIC TAB	<input type="checkbox"/>
Unannounced	<input type="checkbox"/>
Justification	
By _____	
Distribution/	
Availability Codes	
Dist	Avail and/or Special
A-1	



# TABLE OF CONTENTS

<u>SECTION</u>		<u>PAGE</u>
I	INTRODUCTION. . . . .	1
II	DEFINITION OF QUATERNIONS . . . . .	2
III	RIGID BODY DYNAMIC EQUATIONS. . . . .	4
IV	MODEL PROBLEM . . . . .	6
	Nonaxisymmetric Configuration . . . . .	6
	Axisymmetric Configuration. . . . .	7
V	NUMERICAL RESULTS . . . . .	9
	Nonaxisymmetric Configuration . . . . .	9
	Axisymmetric Configuration. . . . .	10
VI	CONCLUSIONS . . . . .	11
	REFERENCES. . . . .	12
	APPENDIX A - ANALYTIC SOLUTION: NONAXISYMMETRIC CASE . . . .	13
	APPENDIX B - ANALYTIC SOLUTION: AXISYMMETRIC CASE. . . . .	20
	FIGURES. . . . .	23

# LIST OF SYMBOLS

$b$	span (feet)
$c$	chord (feet)
$\underline{e}_z$	unit vector along z-axis
$g$	acceleration of gravity (32.2 ft/sec <sup>2</sup> )
$I_x, I_y, I_z$	moments of inertia about the principal axes (foot pounds)
$j$	interger
$k$	function of $\epsilon$
$L, M, N$	aerodynamic moments about body axes (foot pounds)
$m$	aircraft mass (slugs)
$p, q, r$	roll, pitch and yaw rates, respectively (radians/second)
$Q =$	( $q_1, q_2, q_3, q_4$ ) quaternion
$R$	radius (feet)
$s$	scalar of quaternion
$S$	reference area of aircraft (square feet)
$t$	time (seconds)
$u, v, w$	velocity components in body axes (feet per second)
$\underline{V}$	vector of quaternion, velocity vector
$x, y, z$	body axes coordinates
$x_E, y_E, z_E$	inertial axes coordinates
$X, Y, Z$	aerodynamic forces aligned with body axes (pounds)
$\alpha, \beta, \gamma$	angles between rotation axis of quaternion and body axes $x, y, z$ respectively

# LIST OF SYMBOLS (Cont'd)

$\delta^2$	ratio of moments of inertia
$\epsilon$	ratio of initial roll to pitch rate
$\lambda$	trigonometric transformation for pitch rate
$\mu$	rotation angle for quaternion
$\rho$	ambient air density (slugs per cubic foot)
$\psi, \theta, \phi$	Euler angles for azimuth, elevation, and bank respectively
$\underline{\omega}$	rotational velocity vector
$\Omega$	initial pitch or yaw rotation rate (radians per second)
$(\dot{\phantom{x}}) = \frac{d}{dt}$	derivative with respect to time
<u>Subscript</u>	
0	initial value

## SECTION I

### INTRODUCTION

In analyzing aircraft spin and other flight maneuvers with large rotation rates based upon first principles, the non-linear aerodynamic equations (Navier-Stokes) must be coupled with the rigid-body dynamic equations of motion<sup>1,2</sup>. In both systems of equations it is desirable to use a body axes system to describe the forces and moments, and utilize a surface-oriented coordinate system for obtaining the flowfield grid. To solve this system of equations it is necessary to describe the position of the aircraft with respect to a fixed inertial coordinate system. The classic method is to use the Euler angles  $(\phi-\theta-\psi)$  to define the aircraft orientation. However, singularities and ambiguities exist when the elevation angle is plus or minus ninety degrees. This difficulty has been overcome in the field of inertial guidance by the use of quaternions to describe the aircraft position in space<sup>2,3</sup>. It is the purpose of this report to investigate this technique for numerically solving aircraft spin problems. Two problems are addressed; the first is a nonsymmetric body and the second is <sup>a</sup>symmetrical <sup>configuration</sup>. The rotational dynamics and the solution for the quaternions and Euler angles are determined for both problems.

→ p 2



## SECTION II

### DEFINITION OF QUATERNIONS

Hamilton (circa 1840) was the first to point out that the three Euler angles are inadequate to uniquely define the orientation of a body in space and that four variables are required to resolve the predicament. Hence he invented the quaternion, *which*

*A* quaternion is a scalar plus a vector, totalling four elements.

$$\begin{aligned} Q &= s + \underline{v} \\ \text{or} \quad Q &= (q_1, q_2, q_3, q_4) \end{aligned} \quad (1)$$

Three of the elements describe a vector, and this vector defines an axis of rotation. The fourth element, a scalar, defines the magnitude of a rotation angle about the vector axis.

The definition of the four elements of the quaternion follows:

$$\begin{aligned} q_1 &= \cos \frac{\mu}{2} \\ q_2 &= \sin \frac{\mu}{2} \cos \alpha \\ q_3 &= \sin \frac{\mu}{2} \cos \beta \\ q_4 &= \sin \frac{\mu}{2} \cos \gamma \end{aligned} \quad (2)$$

where  $\alpha, \beta, \gamma$  are the angles between the rotation axis and the  $x, y, z$  axis respectively. The amount of rotation is the angle  $\mu$ . The rotations are illustrated in Figure 1.\*

Observe that the quaternions are subject to the constraint that

$$q_1^2 + q_2^2 + q_3^2 + q_4^2 = 1 \quad (3)$$

\* Figures begin on page 23.

The interrelationship with the Euler angles is as follows:

$$\begin{aligned}
 q_1 &= \cos \frac{\psi}{2} \cos \frac{\theta}{2} \cos \frac{\phi}{2} + \sin \frac{\psi}{2} \sin \frac{\theta}{2} \sin \frac{\phi}{2} \\
 q_2 &= \cos \frac{\psi}{2} \cos \frac{\theta}{2} \sin \frac{\phi}{2} - \sin \frac{\psi}{2} \sin \frac{\theta}{2} \cos \frac{\phi}{2} \\
 q_3 &= \cos \frac{\psi}{2} \sin \frac{\theta}{2} \cos \frac{\phi}{2} + \sin \frac{\psi}{2} \cos \frac{\theta}{2} \sin \frac{\phi}{2} \\
 q_4 &= \sin \frac{\psi}{2} \cos \frac{\theta}{2} \cos \frac{\phi}{2} - \cos \frac{\psi}{2} \sin \frac{\theta}{2} \sin \frac{\phi}{2}
 \end{aligned} \tag{4}$$

The relationships for the Euler angles in terms of quaternions are

$$\begin{aligned}
 \sin \theta &= 2(q_1 q_3 - q_2 q_4) \\
 \sin \phi \cos \theta &= 2(q_1 q_2 + q_3 q_4) \\
 \cos \phi \cos \theta &= 1 - 2q_2^2 - 2q_3^2 \\
 \sin \psi \cos \theta &= 2(q_1 q_4 + q_2 q_3) \\
 \cos \psi \cos \theta &= 1 - 2q_3^2 - 2q_4^2
 \end{aligned} \tag{5}$$

The four quaternion position coordinates are computed by solving four differential rate equations.

$$\begin{vmatrix} \dot{q}_1 \\ \dot{q}_2 \\ \dot{q}_3 \\ \dot{q}_4 \end{vmatrix} = \frac{1}{2} \begin{vmatrix} 0 & -p & -q & -r \\ p & 0 & r & -q \\ q & -r & 0 & p \\ r & q & -p & 0 \end{vmatrix} \begin{vmatrix} q_1 \\ q_2 \\ q_3 \\ q_4 \end{vmatrix} \tag{6}$$

where  $p$ ,  $q$ ,  $r$  are the rotation rates in roll, pitch and yaw respectively that must be obtained from the rigid body dynamic equations. These equations are well behaved since  $p$ ,  $q$ , and  $r$  are finite.

### SECTION III

#### RIGID BODY DYNAMIC EQUATIONS

The rigid body dynamic equations used to compute aircraft spin<sup>4</sup> with six degrees of freedom contain three moment equations and three force equations. The selected axes system for the differential equation formulation is a body coordinate frame. This system is selected because the aerodynamic data and the body angular rates are measured relative to it. The x and z axes form a plane of symmetry. It is convenient to align the coordinate system with the principal axes since all products of inertia are zero in this framework.

##### Moment Equations

$$\begin{aligned} I_x \dot{p} + (I_z - I_y)qr &= L(u, v, w, p, q, r, \rho, S, b) \\ I_y \dot{q} + (I_x - I_z)pr &= M(u, v, w, p, q, r, \rho, S, c) \\ I_z \dot{r} + (I_y - I_x)pq &= N(u, v, w, p, q, r, \rho, S, b) \end{aligned} \quad (7)$$

##### Force Equations

$$\begin{aligned} m(\dot{u} + qw - rv) + mg \sin \theta &= X(u, v, w, p, q, r, \rho, S) \\ m(\dot{v} + ru - pw) - mg \sin \phi \cos \theta &= Y(u, v, w, p, q, r, \rho, S) \\ m(\dot{w} + pv - qu) - mg \cos \phi \cos \theta &= Z(u, v, w, p, q, r, \rho, S) \end{aligned} \quad (8)$$

Given the aerodynamic characteristics, along with the mass and inertial parameters, the above six dynamic equations are solved for  $p, q, r, u, v, w$ . The quaternions are obtained by solving Equation (6) as a subroutine in conjunction with the simultaneous solution of Equations (7) and (8).

The hypothesis at this point is that the numerical solution of the quaternion rate Equation (6), is better behaved than the alternative procedure for resolving the Euler angles. The differential equations for the Euler angles are

$$\begin{aligned}\dot{\psi} &= (q \sin \phi + r \cos \phi) \sec \Theta \\ \dot{\Theta} &= q \cos \phi - r \sin \phi \\ \dot{\phi} &= p + \dot{\psi} \sin \Theta\end{aligned}\tag{9}$$

Clearly, difficulties arise when  $\Theta$  reaches plus or minus  $90^\circ$ . The rate for the azimuth angle grows without bound, thus numerical integration of Equation (9) is not possible. But this problem is circumvented by first solving for the quaternions and then the Euler angles from Equations (5).

We next turn our attention to the development of the rotational solution for two problems.

## SECTION IV

### MODEL PROBLEM

#### Nonaxisymmetric Configuration

The first problem was selected to demonstrate the essential features of manipulating the quaternions and to obtain the required numerical experience. Observe that the aerodynamic moments, Equations (7), are coupled to the force equations, Equations (8), through the velocity components. For a situation in which the aerodynamic torque vanishes, the dynamic equations are uncoupled. We will consider such a case, that of a thin rectangular plate which is illustrated in Figure 2(a). In this case, the moments of inertia are also simplified as follows:

$$I_z = I_y + I_x \text{ and } I_y > I_x \quad (10)$$

This example corresponds to a configuration where all products of inertia are zero, which is a fair approximation for most aircraft. For the case of no external torque, it can be shown that rotation about the y vehicle axis with the intermediate value for the moment of inertia ( $I_y$ ) is unstable, while rotation about the other two axes is stable. For this problem the rotation is about the unstable axis.

Equation (7) now reduces to the following simple form:

$$\begin{aligned} \dot{p} + qr &= 0 \\ \dot{q} - pr &= 0 \\ \dot{r} + \delta^2 pq &= 0 \end{aligned} \quad (11)$$

where

$$\delta^2 = \frac{I_y - I_x}{I_y + I_x} < 1 \quad (12)$$

Equation (11) combined with Equation (6) will describe the angular motion of the rigid body given a set of initial conditions. (These values can then be inserted into Equation (8) to find the translational components). Initial conditions for the unstable situation were selected.

$$\begin{aligned} p(0) &= \epsilon \Omega \\ q(0) &= \Omega \\ r(0) &= 0 \\ Q(0) &= (1, 0, 0, 0) \end{aligned} \quad (13)$$

#### Axisymmetric Configuration

The shape for this problem is a thin circular disk with the x and y axes in the circular section and z perpendicular to these axes. The configuration is illustrated in Figure 2(b). All products of inertia are zero. The moments of inertia are

$$\begin{aligned} I_x &= I_y = \frac{1}{4} mR^2 \\ I_z &= \frac{1}{2} mR^2 \end{aligned} \quad (14)$$

where  $R$  is the radius of the disk. The initial rotation is about the  $z$ -axis, thus

$$\begin{aligned} p(0) &= q(0) = 0 \\ r(0) &= \Omega \end{aligned} \tag{15}$$

It is assumed that the aerodynamic moments are zero. Equation (7) reduces to

$$\begin{aligned} \dot{p} + qr &= 0 \\ \dot{q} - pr &= 0 \\ \dot{r} &= 0 \end{aligned} \tag{16}$$

Equations (6) and (16) describe the angular motion of the rigid body, given the initial conditions, Equations (15) and

$$\begin{aligned} \psi(0) &= \phi(0) = 0 \\ \theta(0) &= \theta_0 \end{aligned} \tag{17}$$

From Equation (4), the initial values for the quaternions are

$$Q(0) = \left( \cos \frac{\theta_0}{2}, 0, \sin \frac{\theta_0}{2}, 0 \right) \tag{18}$$

## SECTION V

### NUMERICAL RESULTS

#### Nonaxisymmetric Configuration

The system of equations (Equations (6) and (11)) were solved for parametric values of  $\Omega = 10 \text{ rad/sec}$ ,  $\epsilon = 0.01$  and  $\delta = 0.7$ .

A Runge-Kutta fixed time step integration technique was used.

Figures 3, 4, 5 present the roll, pitch and yaw rates for several revolutions as computed from Equation (11). Figures 6 through 9 present the history of the quaternion position coordinates as determined from Equation (6) using the values of  $p$ ,  $q$ , and  $r$  determined from the solution of Equation (11). The time step size used for the integration was 0.001 sec which was selected after numerical experimentation produced repeatable results. The Euler angles were then computed from Equations (5).

Figures 10 through 12 present the history of the Euler angles. No

difficulty was encountered in numerically integrating Equations (6) and (11). The reason for this is that the quaternions are obtained from Equations (6) which are well behaved. Also, they are bounded by plus and minus one. Thus Equations (11) are well behaved and no difficulty is obtained in integrating them. The difficulty is in attempting to integrate Equations (9). But this is unnecessary since the Euler angles can be obtained directly from Equations (5).

The solutions for the Euler angles  $\psi$  and  $\phi$  undergo rapid transitions. This is a result of two conditions that take place. From Equation (5),  $\theta$  approaches plus or minus  $90^\circ$  and the combination of the quaternions on the right side changes sign. Thus the right side changes rapidly from large positive values to large negative values and vice versa.



A further observation is that the rotational rates are periodic functions of time. But the Euler angles are not.

An analytical solution to this problem exists (see Appendix A). Excellent agreement was obtained between the numerical and analytical values thereby confirming the numerical approach.

#### Axisymmetric Configuration

The system of equations, Equations (6) and (16) were solved for a parametric yaw rate of  $\Omega = 10$  rad/sec. It is shown in Appendix B and can be verified numerically that the solution for the body angular rates is

$$\begin{aligned} p &= 0 \\ q &= 0 \\ r &= \Omega \end{aligned} \tag{19}$$

Figures 13 through 16 are the time histories of the quaternions. Figures 17 through 19 are the Euler angles.

Two significant results are established in Appendix B. The first is that the configuration remains in the same vertical plane that it started in whenever the bank angle is zero. The second result is that the attitude does not change throughout the trajectory. These results agree with the observed trajectory of a Frisbee when the initial bank angle is zero. The numerical solution agrees with the analytical solution of Appendix B.

## SECTION VI

### CONCLUSIONS

Experience has shown that numerical difficulties arise in using the Euler angles to describe the orientation of an aircraft during large changes in the Euler elevation angle. The angular rates for the heading and bank angles are undefined whenever the elevation angle reaches plus or minus ninety degrees. The numerical difficulties may be completely overcome through the use of quaternions in place of the Euler angles. The Euler angles are then easily computed from the quaternion solution.

Two problems were solved numerically and analytically. The results for the two approaches did agree and there was no difficulty in obtaining numerical results. The first problem was an example of a nonaxisymmetric configuration. The rotation was about the unstable principal axis. The body rotational rates were periodic, however, the quaternions and Euler angles were not.

The second problem represented an axisymmetric configuration. Again no numerical difficulties were obtained when the quaternions were used. The rotation was about the yaw axis. Two significant results obtained were that if the initial bank angle was zero, then the trajectory remained in the initial vertical plane. The second result was that the attitude did not change throughout the trajectory. The use of quaternions to solve flight mechanics problems is therefore highly recommended for future investigations.

## REFERENCES

1. Galloway, C., "Numerical Computation of an Autorotating Plate," PhD Dissertation, AFIT/DS/AA/83-1, WPAFB, OH (to be published).
2. Robinson, A.C., "On the Use of Quaternions in Simulation of Rigid Body Motion," WADC TR 58-17, Dec 1958, USAF, Wright Air Development Center, WPAFB, OH.
3. Ickes, B.P., "A New Method for Performing Digital Control System Attitude Computations Using Quaternions," AIAA Journal, Vol. 8, No. 1, Jan 1970.
4. Etkin, B., Dynamics of Atmospheric Flight, New York, Wiley, 1972.
5. Byrd, P.F., and Friedman, M.D., Handbook of Elliptic Integrals for Engineers and Physicists, Springer-Verlag, 1954.
6. Selby, S.M., CRC Standard Mathematical Tables, Student Edition, 18th Edition, The Chemical Rubber Co, 1970.

## APPENDIX A

### ANALYTIC SOLUTION: NONAXISYMMETRIC CASE

An analytic solution exists for the model problem selected.

$$\begin{aligned} \dot{p} + qr &= 0 & p(0) &= \epsilon \Omega \\ \dot{q} - pr &= 0 & q(0) &= \Omega \\ \dot{r} + \delta^2 pq &= 0 & r(0) &= 0 \end{aligned} \tag{A-1}$$

Regroup these three moment equations as follows:

$$\begin{aligned} \dot{p} &= -qr = -q\dot{q}/p & \text{or} & \quad \frac{d}{dt} (p^2 + q^2) = 0 \\ \dot{q} &= pr = -r\dot{r}/\delta^2 q & \text{or} & \quad \frac{d}{dt} (r^2 + \delta^2 q^2) = 0 \\ \dot{r} &= -\delta^2 pq = \delta^2 p\dot{p}/r & \text{or} & \quad \frac{d}{dt} (\delta^2 p^2 - r^2) = 0 \end{aligned} \tag{A-2}$$

These three equations may be integrated readily and evaluated using the initial conditions. Hence,

$$\begin{aligned} p^2 + q^2 &= \Omega^2 (1 + \epsilon^2) \\ q^2 + r^2/\delta^2 &= \Omega^2 \\ p^2 - r^2/\delta^2 &= \epsilon^2 \Omega^2 \end{aligned} \tag{A-3}$$

These expressions are energy constraint relationships, however, only two independent equations are evident with the third one being redundant. Therefore, one additional differential equation must be solved and the two energy constraints used to obtain the complete solution.

Differentiate Equation (11) with respect to time.

$$\begin{aligned} \ddot{p} &= -\dot{q}r - \dot{r}q = -p(r^2 - \delta^2 q^2) \\ \ddot{q} &= \dot{r}p + \dot{p}r = -q(r^2 + \delta^2 p^2) \\ \ddot{r} &= -\delta^2 \dot{p}q - \delta^2 \dot{q}p = \delta^2 r(q^2 - p^2) \end{aligned} \tag{A-4}$$

The energy constraints of Equation (A-3) may be inserted into one of the above equations to obtain a single differential equation with one dependent variable.

We will select the middle equation.

$$\ddot{q} + 2\delta^2[(1+\epsilon^2/2)\Omega^2 - q^2]q = 0 \quad (\text{A-5})$$

This equation is called "Duffings Equation" and possesses an analytic solution. The solution is obtained as follows:

Observe that

$$\ddot{q} = \frac{d\dot{q}}{dt} = \dot{q} \frac{d\dot{q}}{dq} = 1/2 \frac{d\dot{q}^2}{dq} \quad (\text{A-6})$$

Hence Equation (A-6) becomes:

$$d\dot{q}^2 = -4\delta^2[(1+\epsilon^2/2)\Omega^2 - q^2]q dq \quad (\text{A-7})$$

Equation (A-7) may be immediately integrated once

$$\dot{q}^2 = \delta^2 q^2 [q^2 - (2+\epsilon^2)\Omega^2] + C_1 \quad (\text{A-8})$$

The initial conditions may be used to evaluate  $C_1$

$$\begin{aligned} \dot{q}(0) &= p(0) \quad r(0) = 0 \\ q(0) &= \Omega \end{aligned} \quad (\text{A-9})$$

Hence

$$C_1 = \delta^2(1+\epsilon^2)\Omega^4 \quad (\text{A-10})$$

Equation (A-8) then becomes

$$\dot{q}^2 = \delta^2(\Omega^2 - q^2) [\Omega^2(1+\epsilon^2) - q^2] \quad (\text{A-11})$$

Solving for  $\dot{q}$  gives

$$\dot{q} = \pm \delta \sqrt{\Omega^2 - q^2} \sqrt{\Omega^2(1+\epsilon^2) - q^2} \quad (\text{A-12})$$

The sign is determined as follows: Initially

$$\begin{aligned} q(0) &= \Omega > 0 \\ \dot{q}(0) &= 0 \\ \ddot{q}(0) &= -q(0) \delta^2 p^2(0) < 0 \end{aligned} \quad (\text{A-13})$$

Thus in the neighborhood of  $t=0$ ,  $q$  is a convex function. It follows that for  $t>0$ ,  $\dot{q}<0$  and therefore the negative sign is selected.

$$\dot{q} = -\delta\sqrt{\Omega^2 - q^2} \sqrt{\Omega^2(1+\epsilon^2) - q^2} \quad (\text{A-14})$$

A convenient transformation is next employed. Let

$$\sin \lambda = \frac{q}{\Omega} \quad (\text{A-15})$$

Differentiating gives

$$\cos \lambda \frac{d\lambda}{dt} = \frac{\dot{q}}{\Omega} \quad (\text{A-16})$$

Since

$$\lambda(0) = \pi/2 \quad (\text{A-17})$$

and  $q$  decreases with time

$$\lambda(t) \leq \pi/2 \quad (\text{A-18})$$

Equation (A-16) can be written as

$$\dot{q} = \sqrt{\Omega^2 - q^2} \cdot \dot{\lambda} \quad (\text{A-19})$$

Equating to Equation (A-14) gives

$$\dot{\lambda} = -\frac{\delta\Omega}{k} \sqrt{1 - k^2 \sin^2 \lambda} \quad (\text{A-20})$$

where

$$k^{-2} = 1 + \epsilon^2 \quad (\text{A-21})$$

Equation (A-20) can be integrated

$$-\frac{\delta\Omega}{k} t = \int_{\pi/2}^{\lambda} \frac{d\lambda}{\sqrt{1 - k^2 \sin^2 \lambda}} \quad (\text{A-22})$$

Rewrite the right side

$$-\frac{\delta\Omega}{k} t = -\int_0^{\pi/2} \frac{d\lambda}{\sqrt{1-k^2 \sin^2 \lambda}} + \int_0^{\lambda} \frac{d\lambda}{\sqrt{1-k^2 \sin^2 \lambda}} \quad (\text{A-23})$$

Both integrals are elliptic integrals of the first kind.<sup>5</sup> Let

$$F(\lambda, k) = \int_0^{\lambda} \frac{d\lambda}{\sqrt{1-k^2 \sin^2 \lambda}} \quad (\text{A-24})$$

then

$$\frac{\delta\Omega}{k} t = F(\pi/2, k) - F(\lambda, k) \quad (\text{A-25})$$

For the example problem,  $k$  is near unity, therefore from Reference 5

$$F(\pi/2, k \rightarrow 1) \rightarrow \ln \frac{4}{\sqrt{1-k^2}} \rightarrow \ln \frac{4}{\epsilon} \quad (\text{A-26})$$

A table for the solution follows for a  $k = 0.99995$

$\lambda$	$F(\lambda, k)$	$\delta/\Omega$	$\frac{\delta \Omega t}{k}$
90°	5.991	1.000	0
85°	3.126	.996	2.865
80°	2.436	.985	3.555
70°	1.735	.940	4.256
60°	1.317	.866	4.674
50°	1.011	.766	4.980
40°	.763	.643	5.228
30°	.549	.500	5.442
20°	.356	.342	5.635
10°	.175	.174	5.816
0°	0	0	5.991

The relations for  $p$  and  $r$  are determined in a manner similar to the way that  $q$  was determined. Initially

$$\dot{p}(0) = 0$$

$$\ddot{p}(0) = p(0)\delta^2 q^2(0) > 0$$

(A-27)

$$\dot{r}(0) < 0$$

In the neighborhood of  $t=0$ ,  $p$  is a concave function and  $r$  is a decreasing function. From Equation (A-3)

$$p = \pm \sqrt{\Omega^2(1+c^2)-q^2}$$

(A-28)

$$= \pm \frac{\Omega}{k} \sqrt{1-k^2 \sin^2 \lambda}$$



Since  $p$  increases

$$p = \frac{\Omega}{k} \sqrt{1 - k^2 \sin^2 \lambda} \quad (\text{A-29})$$

From Equation A-3

$$\begin{aligned} r &= \pm \delta \sqrt{\Omega^2 - q^2} \\ &= \pm \delta \Omega \cos \lambda \end{aligned} \quad (\text{A-30})$$

From the initial boundary condition and  $\dot{r}(0) < 0$ , it follows that

$$r = - \delta \Omega \cos \lambda \quad (\text{A-31})$$

The following table presents the numerical values obtained by numerical integration.

$t$ (sec)	$P$ (rad/sec)	$\dot{\theta}$ (rad/sec)	$\dot{r}$ (rad/sec)
0	0.10	10.00	0
.409	0.88	9.96	-0.61
.508	1.74	9.85	-1.22
.608	3.42	9.40	-2.39
.668	5.01	8.66	-3.50
.711	6.41	7.68	-4.49
.747	7.66	6.42	-5.36
.777	8.65	5.02	-6.05
.805	9.40	3.42	-6.58
.831	9.85	1.73	-6.90
.856	10.00	0	-7.00

The agreement between the theoretical values for the body rotational rates and those obtained by numerical integration of the differential equations is very good. This can be observed by comparing the tabular results with Figures 3, 4, and 5. Observe that the "rate period" is

$$\text{Period} = \frac{4k}{\delta\Omega} F(\pi/2, k) = 3.423 \text{ sec} \quad (\text{A-32})$$

Note that the range may be extended as follows for any integer  $j$ :

$$F(j\pi \pm \lambda, k) = 2jF(\pi/2, k) \pm F(\lambda, k) \quad (\text{A-33})$$

and

$$F(-\lambda, k) = -F(\lambda, k) \quad (\text{A-34})$$

## APPENDIX B

### ANALYTIC SOLUTION: AXISYMMETRIC CASE

The body angular rates satisfy

$$\begin{aligned} \dot{p} + qr &= 0 & p(0) &= 0 \\ \dot{q} - rp &= 0 & q(0) &= 0 \\ \dot{r} &= 0 & r(0) &= \Omega \end{aligned} \quad (B-1)$$

From the latter equation

$$r = \Omega \quad (B-2)$$

Combining the first two equations gives

$$\ddot{p} = -\dot{q}r = -r^2 p \quad (B-3)$$

The boundary conditions are

$$p(0) = \dot{p}(0) = 0 \quad (B-4)$$

The solution is

$$p=0 \quad (B-5)$$

In a similar way, it can be concluded that

$$q=0 \quad (B-6)$$

Substitution of  $p, q$ , and into Equation 5 gives

$$\begin{aligned} \dot{q}_1 &= -\frac{1}{2} r q_4 \\ \dot{q}_2 &= \frac{1}{2} r q_3 \\ \dot{q}_3 &= -\frac{1}{2} r q_2 \\ \dot{q}_4 &= \frac{1}{2} r q_1 \end{aligned} \quad (B-7)$$

Combining the first and last equations gives

$$\ddot{q}_1 = -\left(\frac{1}{2}\Omega\right)^2 q_1 \quad (B-8)$$

Analytic integration using the boundary conditions gives

$$q_1 = \cos \frac{\theta_0}{2} \cos \frac{\Omega t}{2} \quad (B-9)$$

$q_4$  can be obtained directly from the first differential equation

$$q_4 = -\frac{2}{r} \dot{q}_1 = \cos \frac{\theta_0}{2} \sin \frac{\Omega t}{2} \quad (B-10)$$

Combining the second and third differential equations results in a second-order differential equation. Integrating and satisfying the boundary conditions gives

$$\begin{aligned} q_2 &= \sin \frac{\theta_0}{2} \sin \frac{\Omega t}{2} \\ q_3 &= \sin \frac{\theta_0}{2} \cos \frac{\Omega t}{2} \end{aligned} \quad (B-11)$$

The Euler angles are obtained from Equation (14)

$$\begin{aligned} \sin \theta &= 2(q_1 q_3 - q_2 q_4) = \sin \theta_0 \cos \Omega t \\ \sin \phi &= 2(q_1 q_2 + q_3 q_4) \sec \theta = \sin \theta_0 \sin \Omega t \sec \theta \\ \cos \phi &= (1 - 2q_2^2 - 2q_3^2) \sec \theta = \cos \theta_0 \sec \theta \\ \sin \psi &= 2(q_2 q_3 + q_1 q_4) \sec \theta = \sin \Omega t \sec \theta \\ \cos \psi &= (1 - 2q_3^2 - 2q_4^2) \sec \theta = \cos \theta_0 \cos \Omega t \sec \theta \end{aligned} \quad (B-12)$$

Let the inertial coordinate axes be defined as follows: The  $x_E$  and  $z_E$  axes are in the vertical plane of the initial motion. The  $y_E$  axis is perpendicular to these axes. The kinematic relation for  $y_E$  in terms of the quaternions and velocity components is

$$\begin{aligned} \dot{y}_E &= 2u(q_1 q_4 + q_2 q_3) + v(1 - 2q_2^2 - 2q_4^2) + 2w(q_3 q_4 - q_1 q_2) \\ &= u \sin \Omega t + v \cos \Omega t \end{aligned} \quad (B-13)$$

Let  $V_p$  denote the component of the velocity vector measured in the x-y plane. Then the components  $u$  and  $v$  satisfy

$$\begin{aligned} u &= V_p \cos \Omega t \\ v &= -V_p \sin \Omega t \end{aligned} \quad (B-14)$$

These two equations follow from the result that the x and y axes are rotating at a constant rate  $\Omega$ . Substitution of u and v into  $\dot{y}_E$  gives  $\dot{y}_E=0$ . Therefore  $y_E$  is equal to its initial result and does not move out of the  $x_E$ - $z_E$  plane.

Since p and q are zero, the angular velocity of the x,y,z coordinate frame is  $\underline{\omega}$  where

$$\underline{\omega} = r \underline{e}_z \quad (B-15)$$

The rate of change of  $\underline{e}_z$  is determined from

$$\frac{d}{dt} \underline{e}_z = \underline{\omega} \times \underline{e}_z = r \underline{e}_z \times \underline{e}_z = 0 \quad (B-16)$$

Therefore  $\underline{e}_z$  which lies along the z-axis does not change. Consequently the orientation of the z-axis does not change. The conclusion is that the attitude does not change.

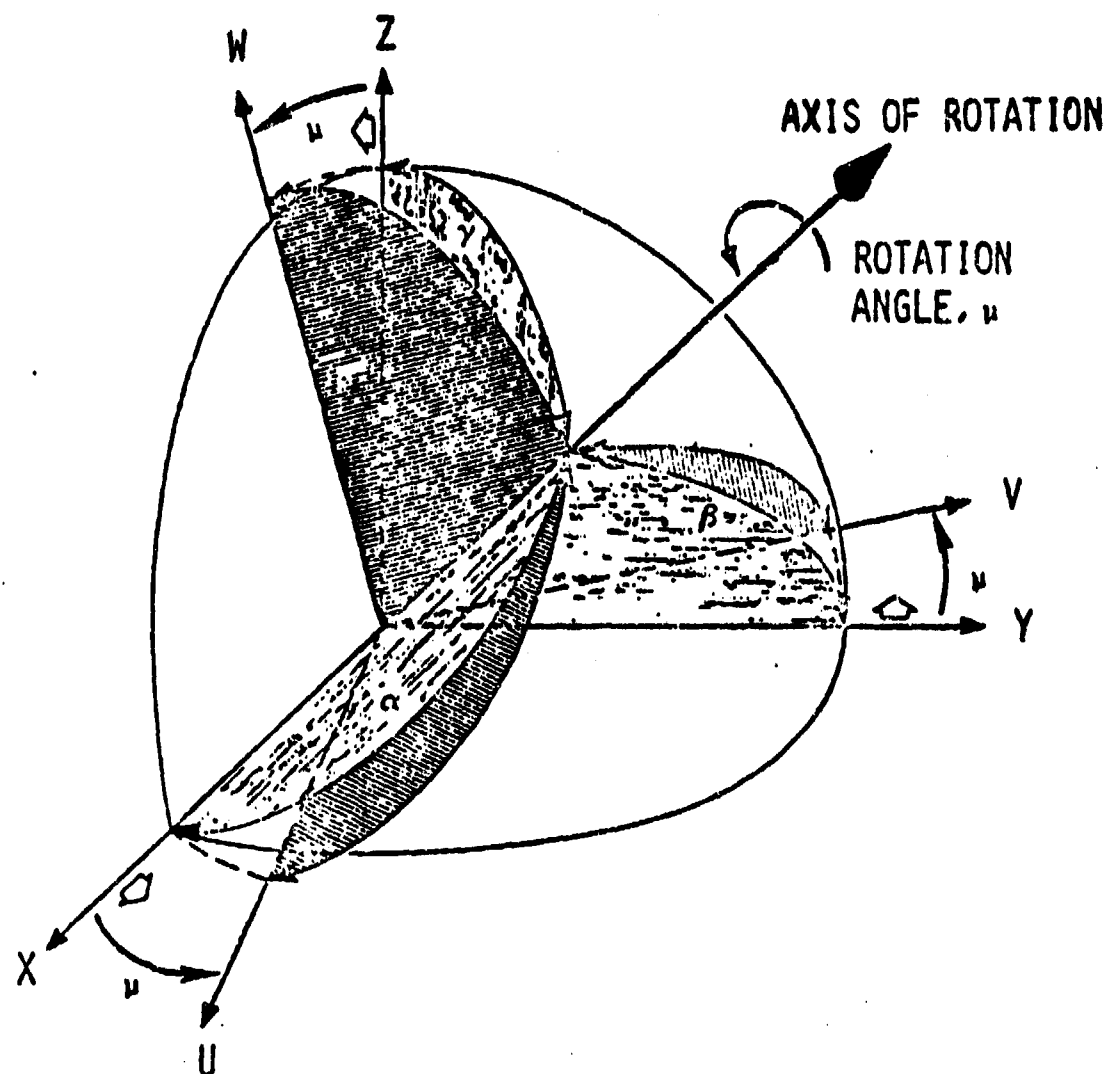
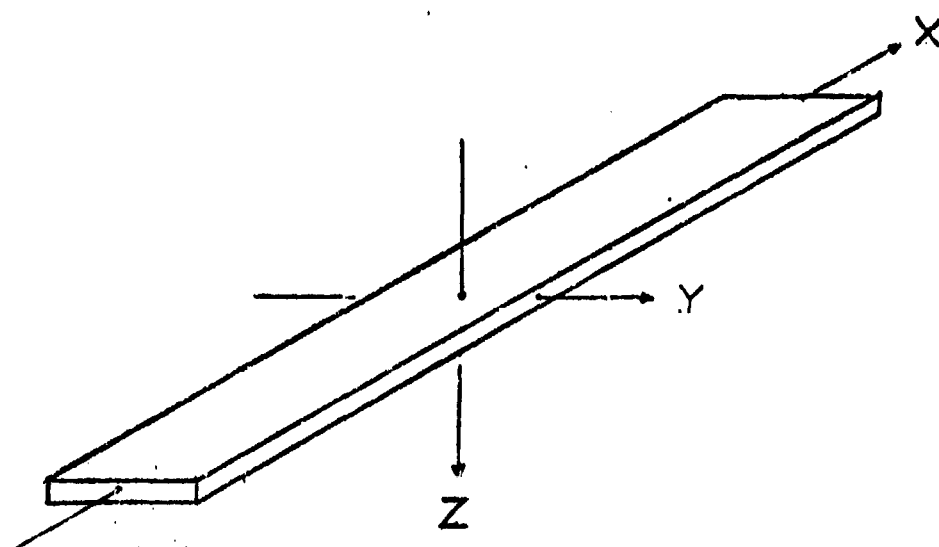
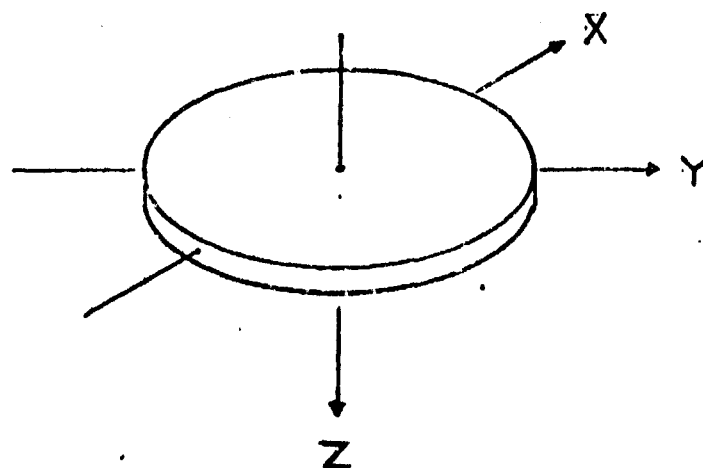


Figure 1 Angular Transformations



NON AXISYMMETRIC CONFIGURATION



AXISYMMETRIC CONFIGURATION

Figure 2 Model Configurations

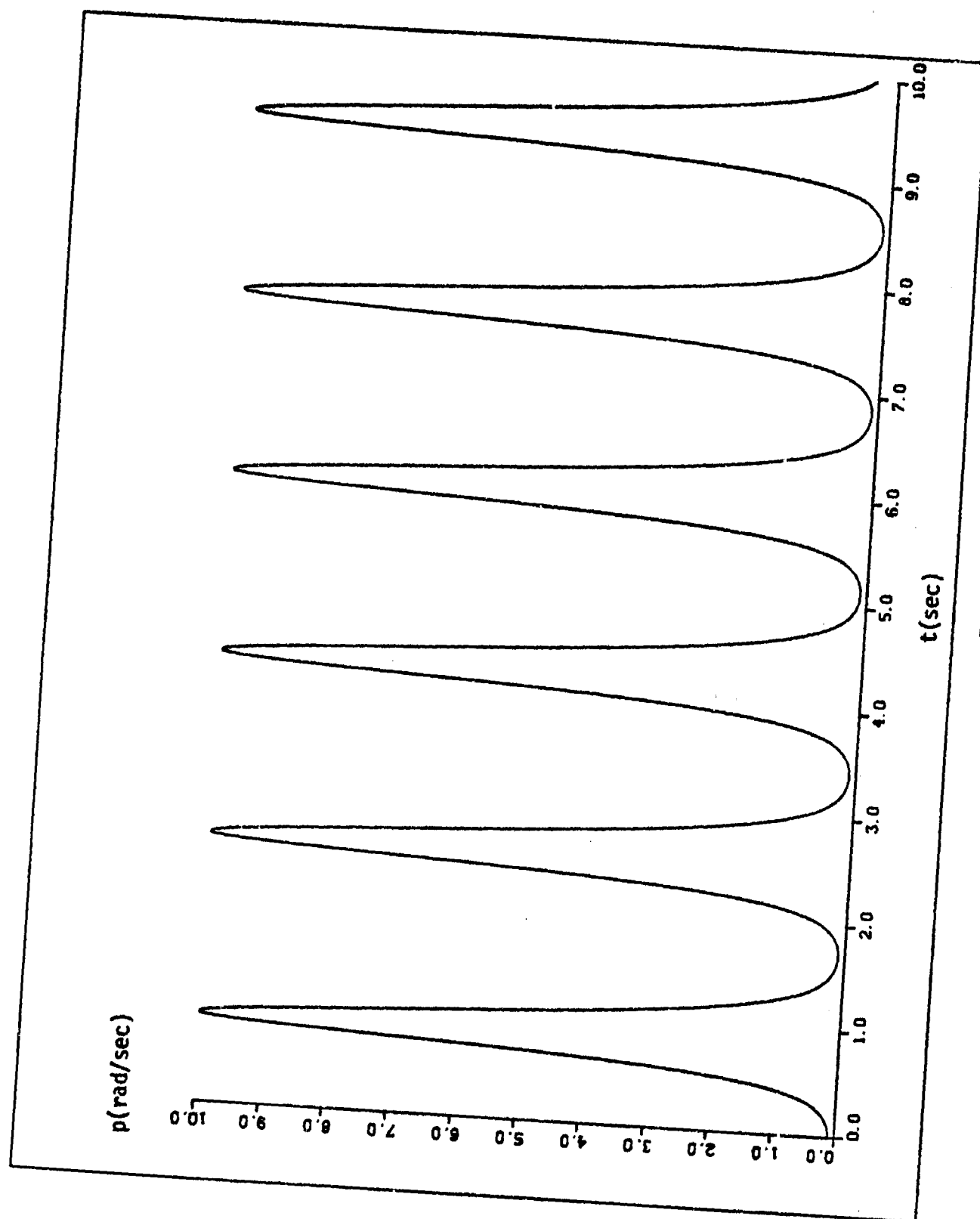


Figure 3 Roll Rate



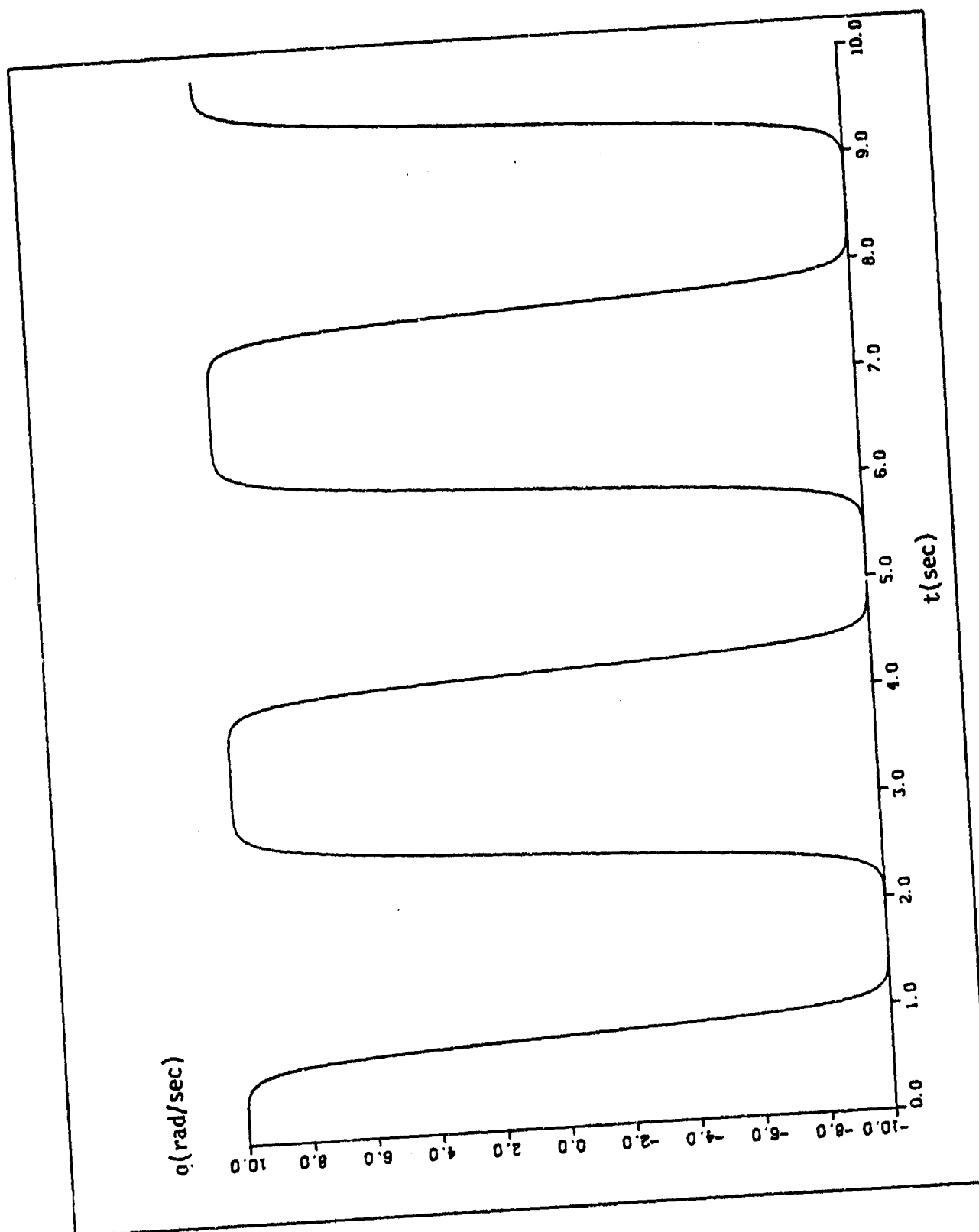


Figure 4 Pitch Rate

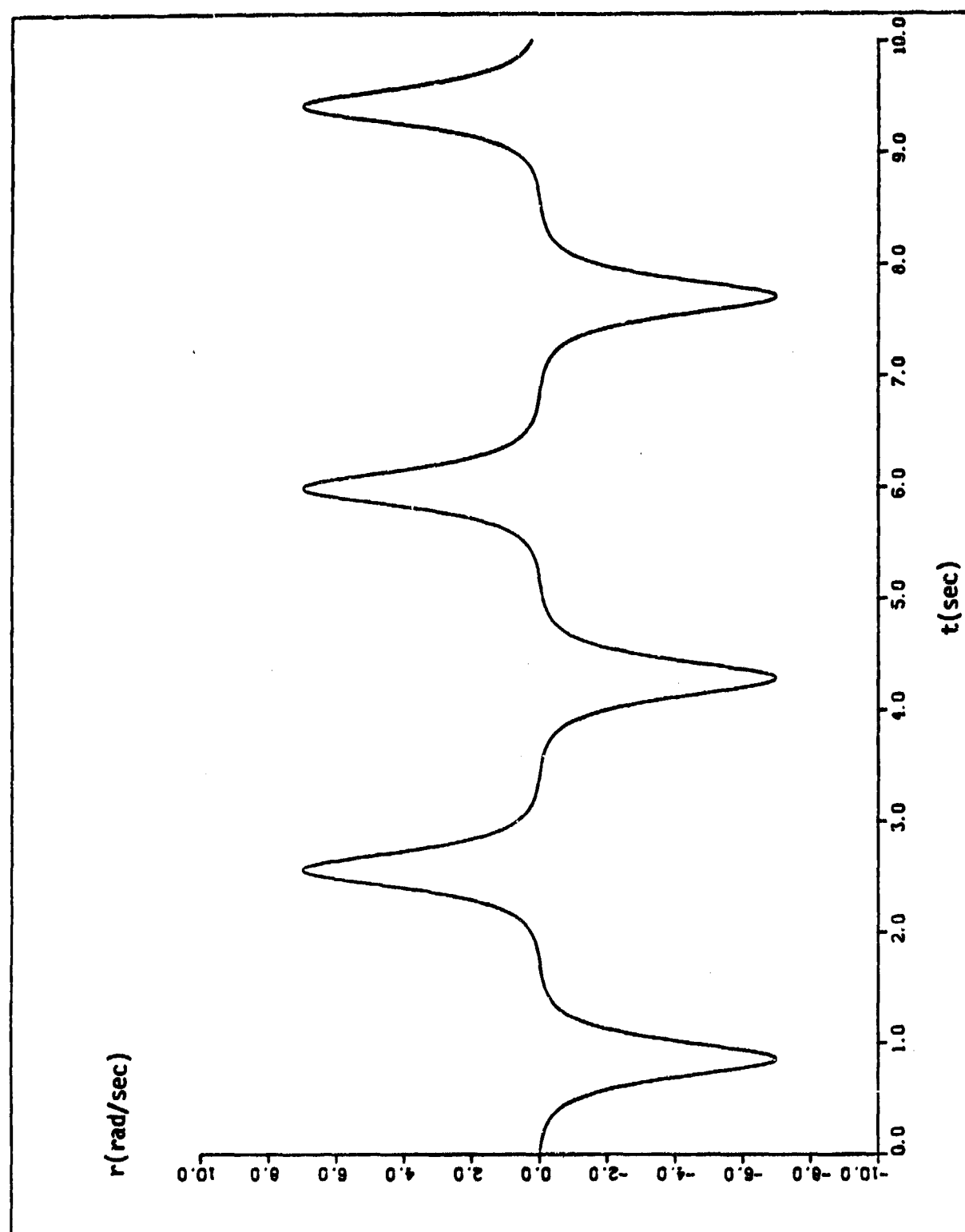


Figure 5 Yaw Rate

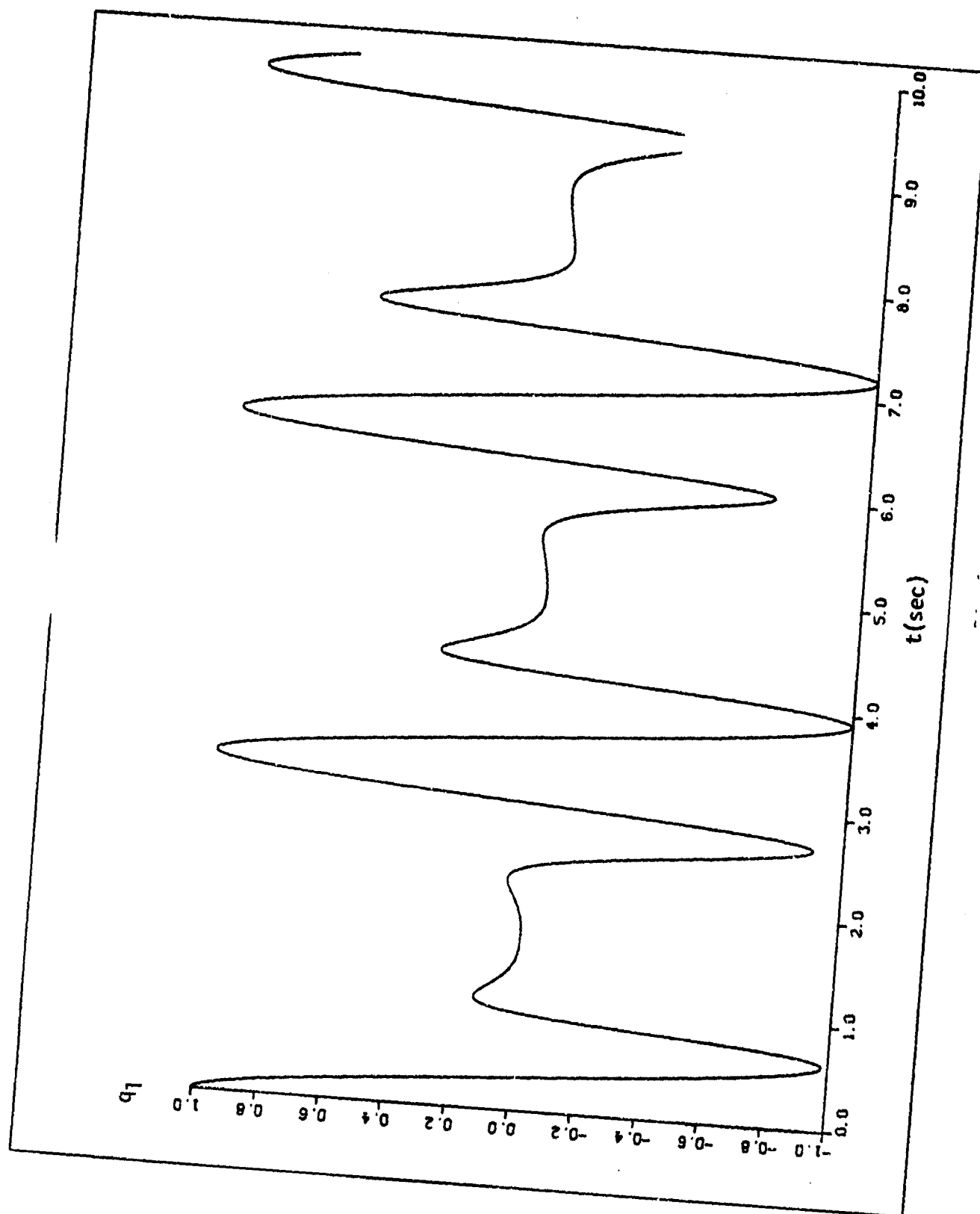


Figure 6  $q_1$  Quaternion

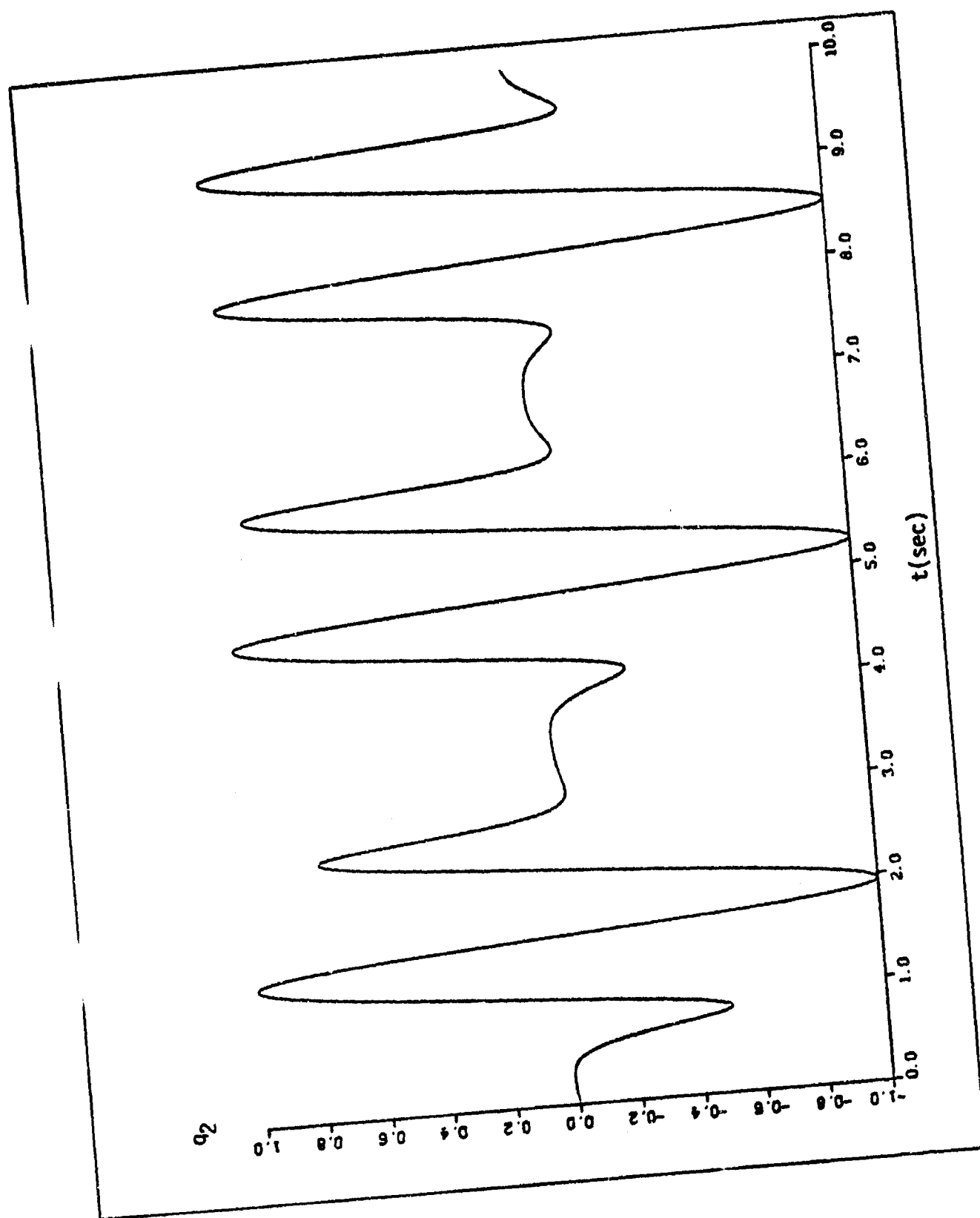


Figure 7  $q_2$  Quaternion

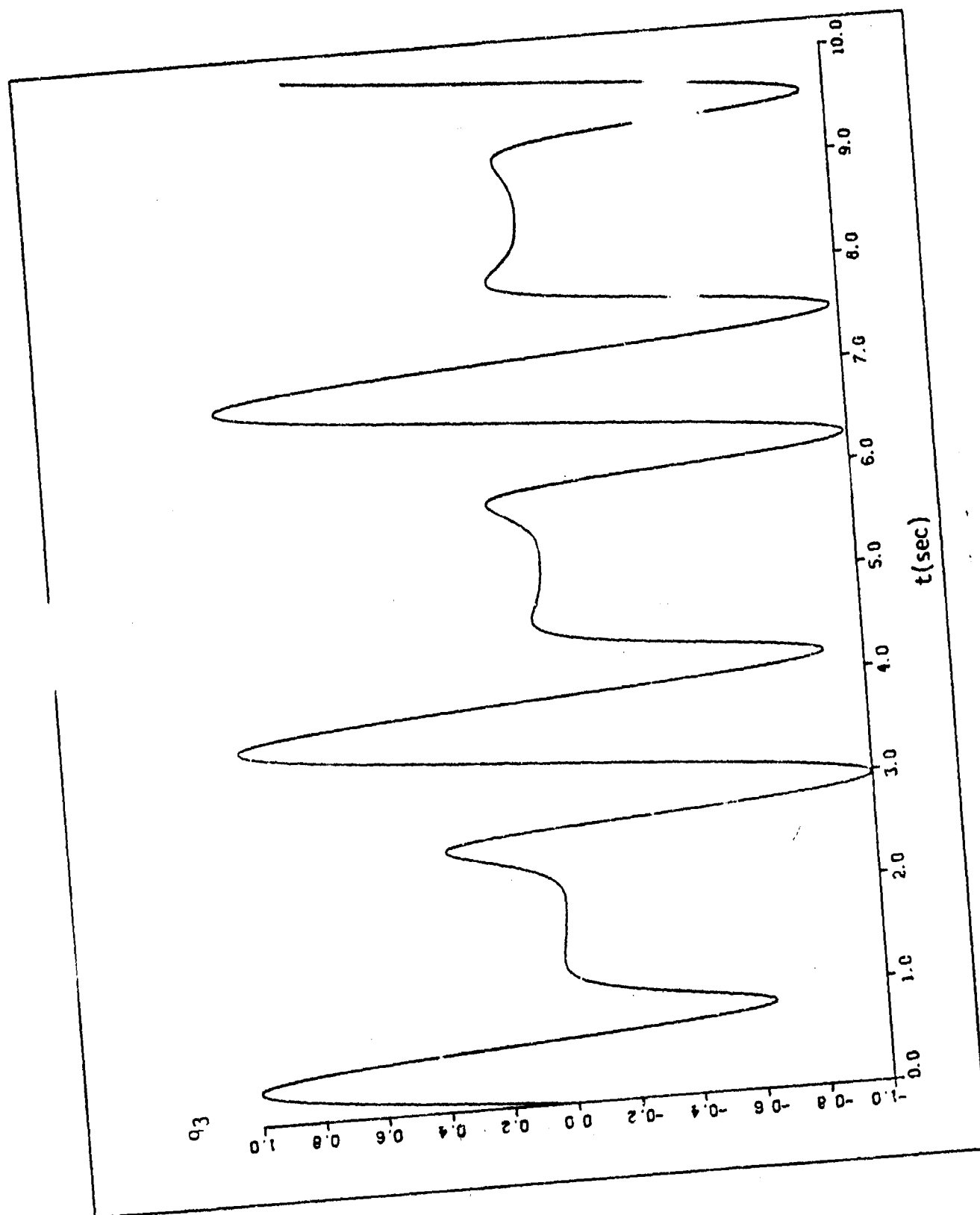


Figure 8  $q_3$  Quaternion

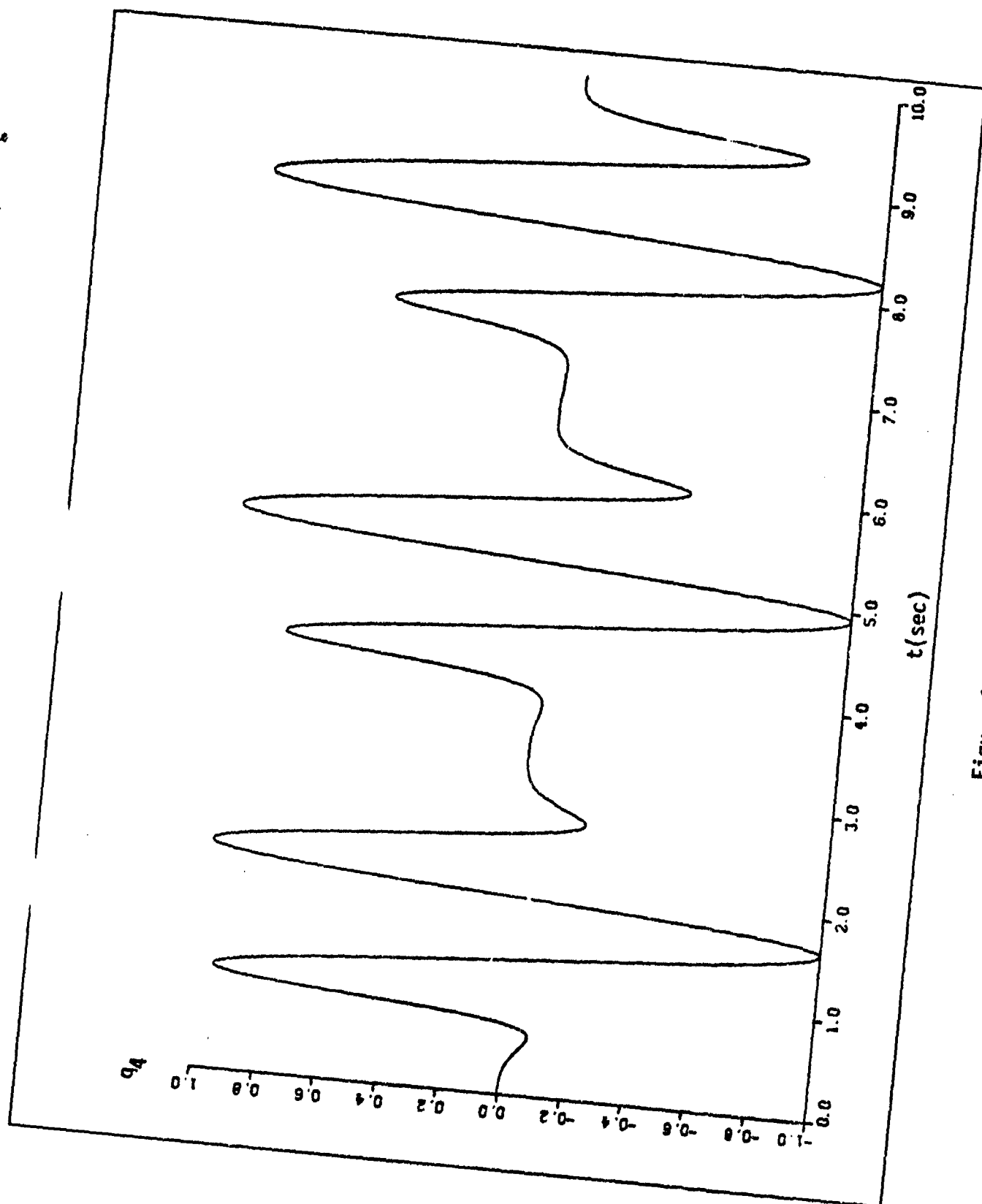


Figure 9  $q_4$  Quaternion

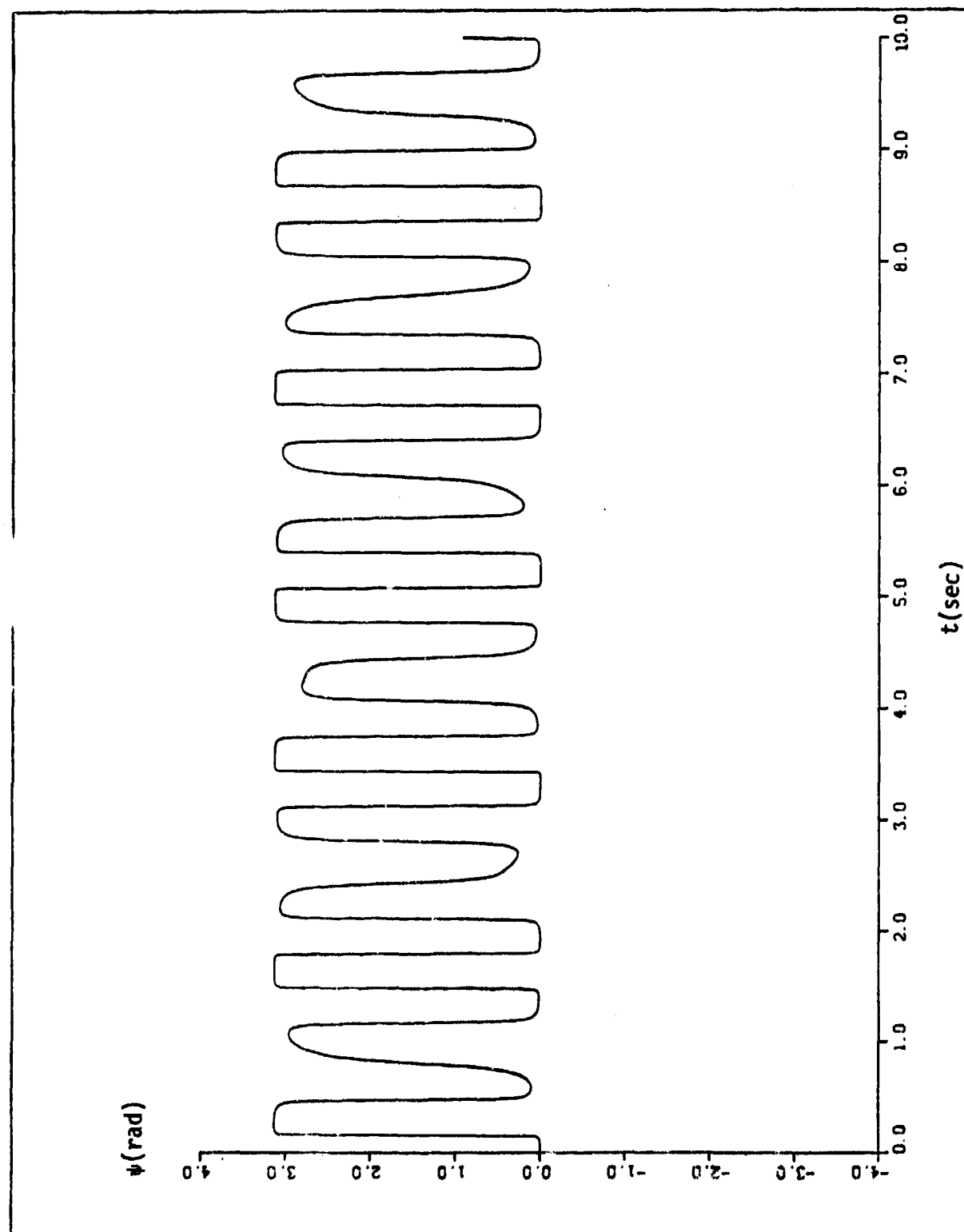


Figure 10 Euler Azimuth Angle

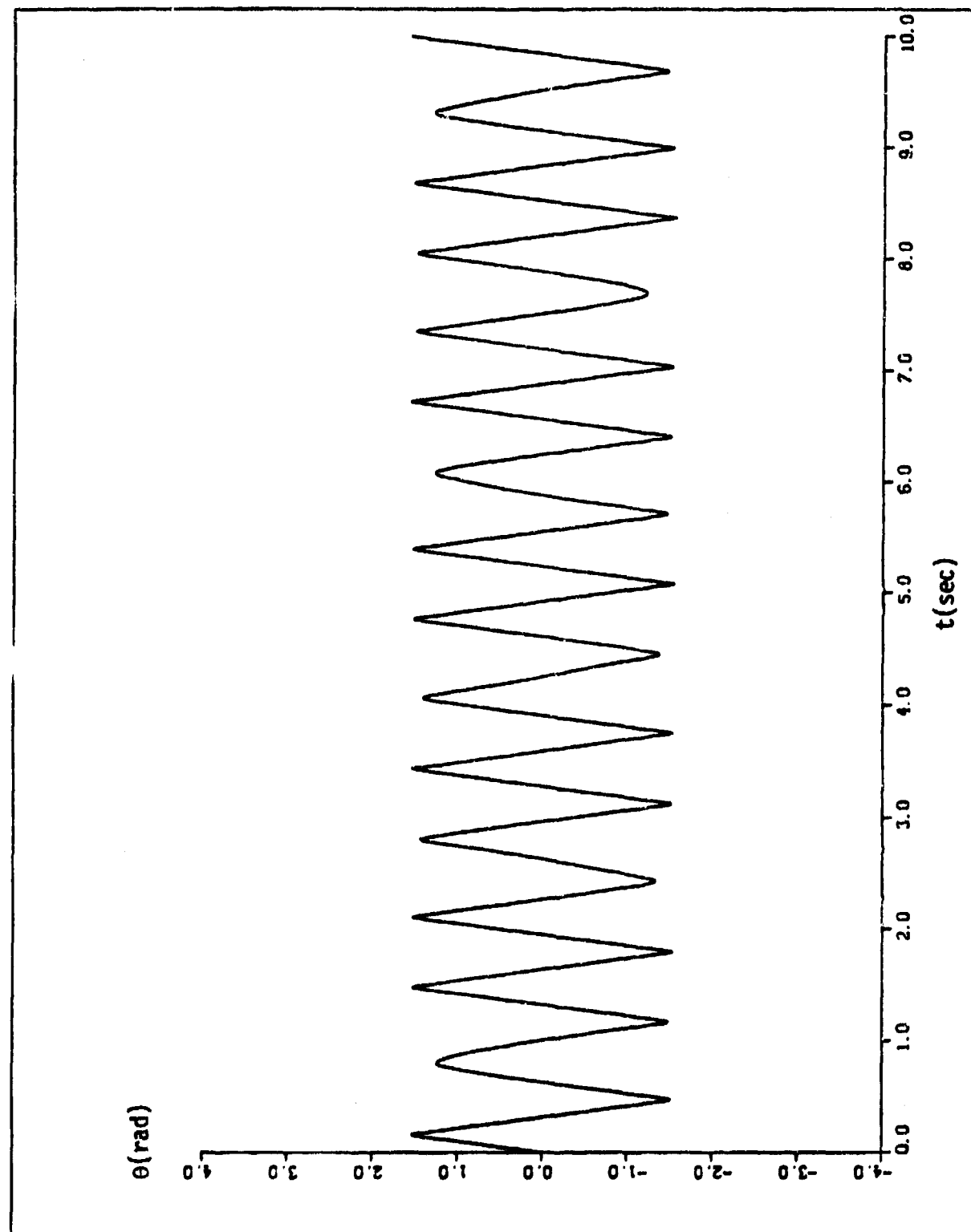


Figure 11 Euler Elevation Angle



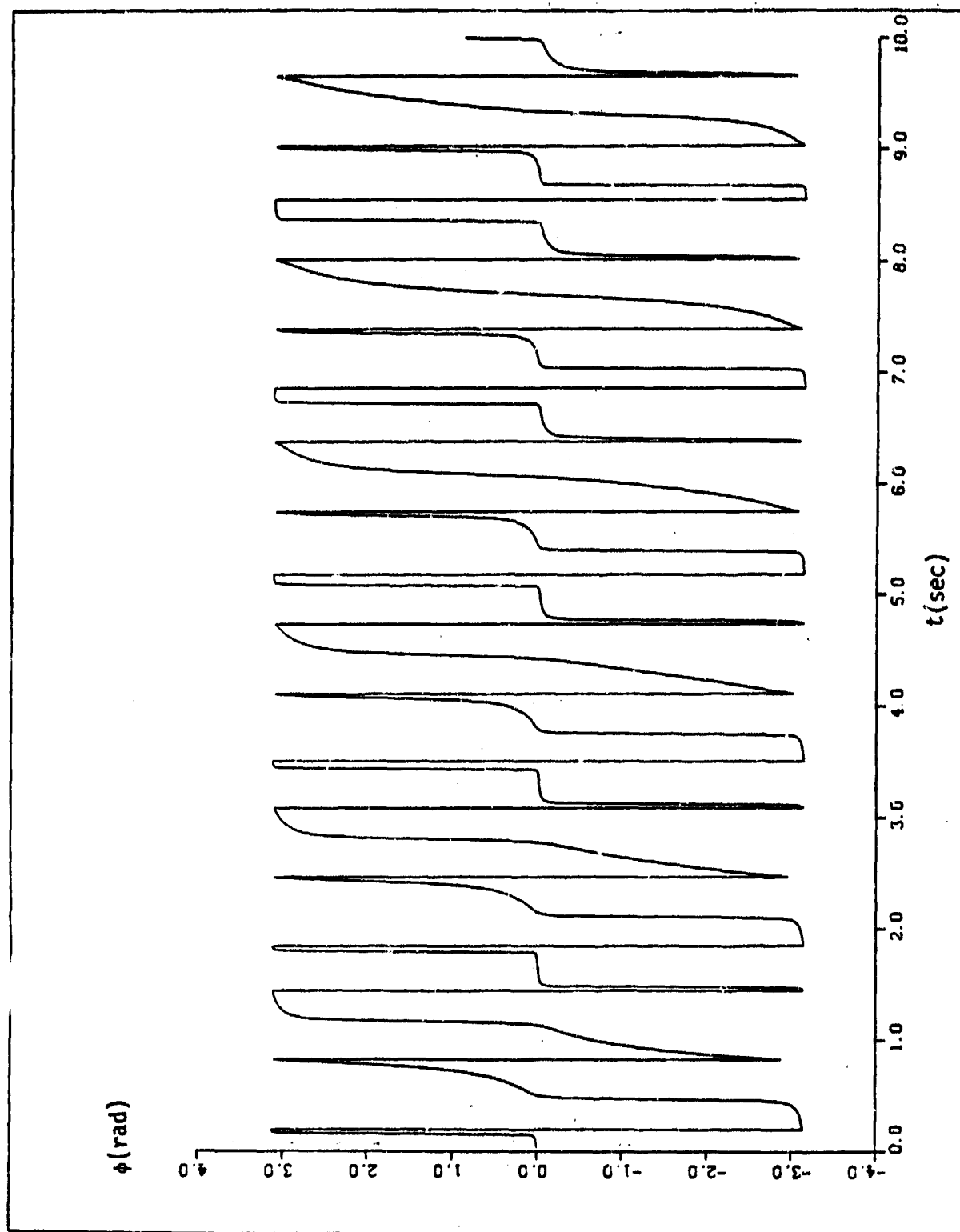


Figure 12 Euler Bank Angle

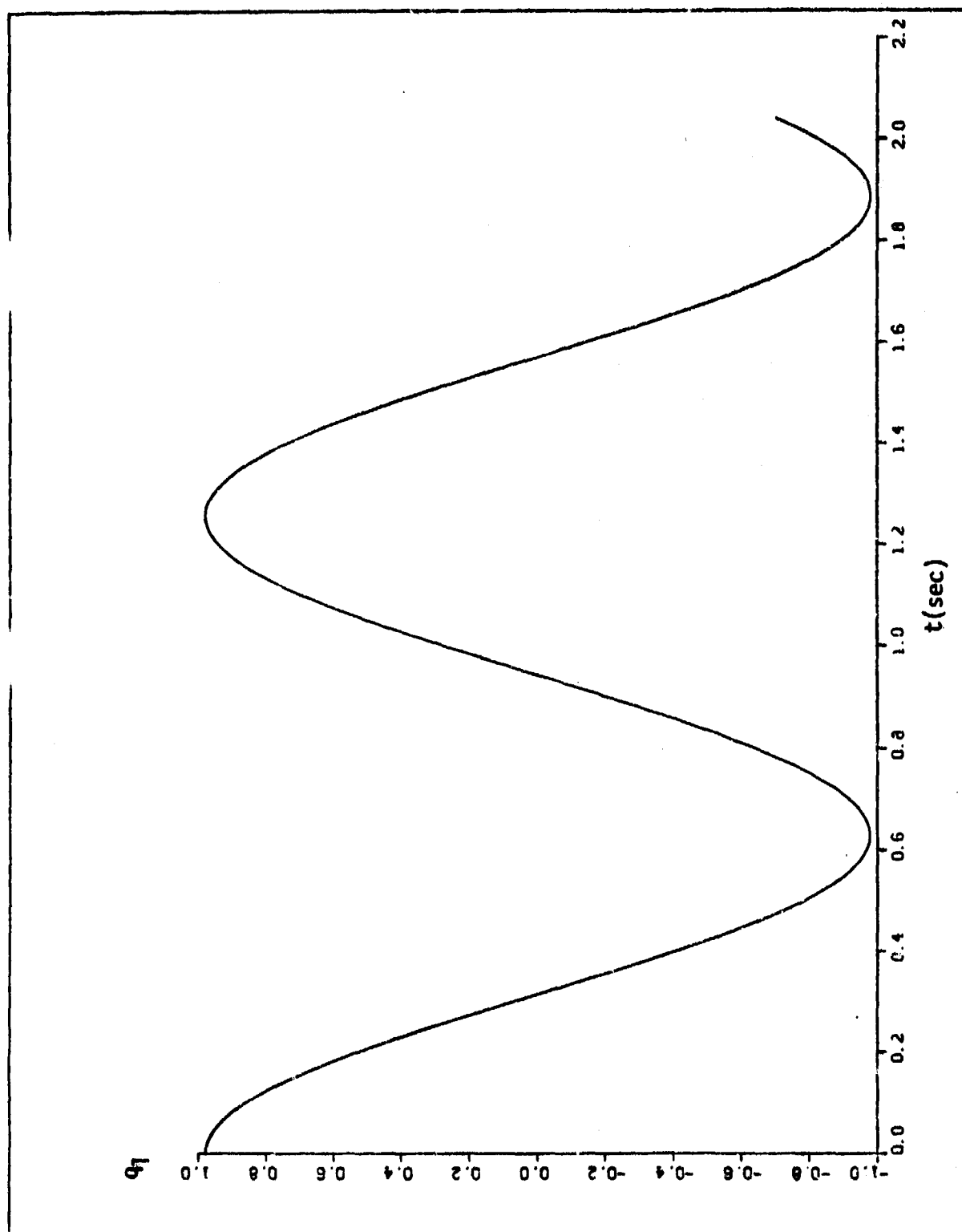


Figure 13  $q_1$  Quaternion

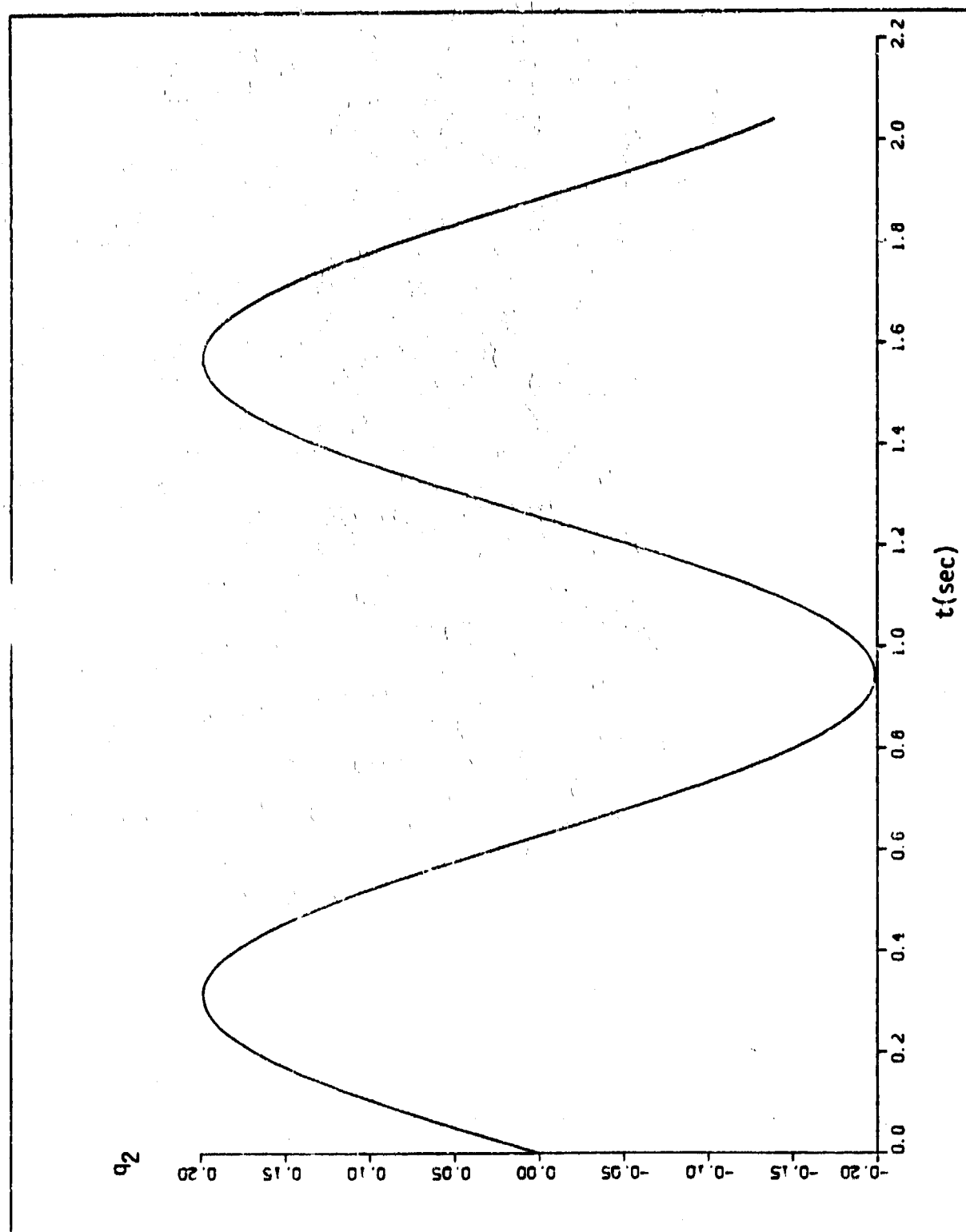


Figure 14  $q_2$  Quaternion

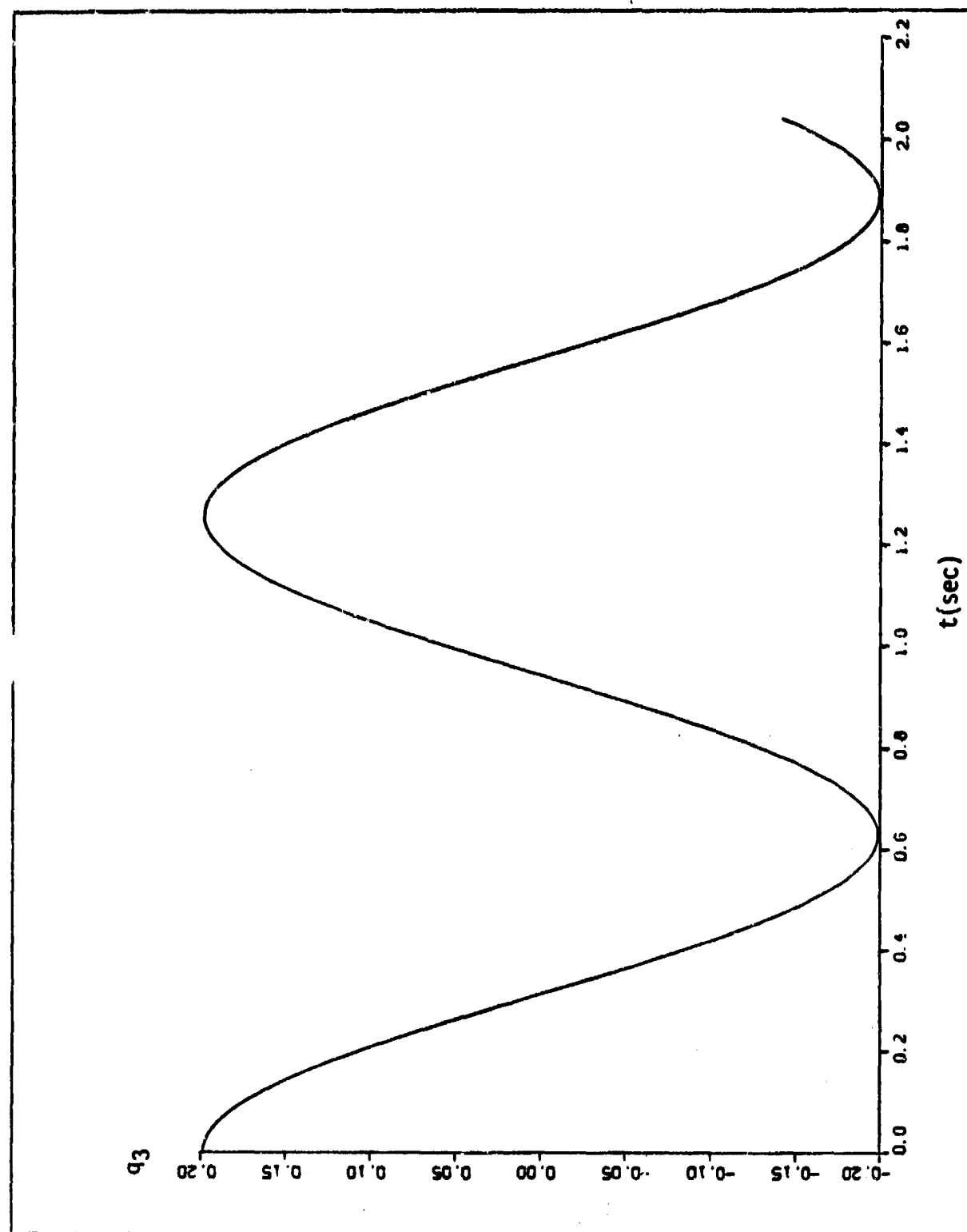


Figure 15  $q_3$  Quaternion

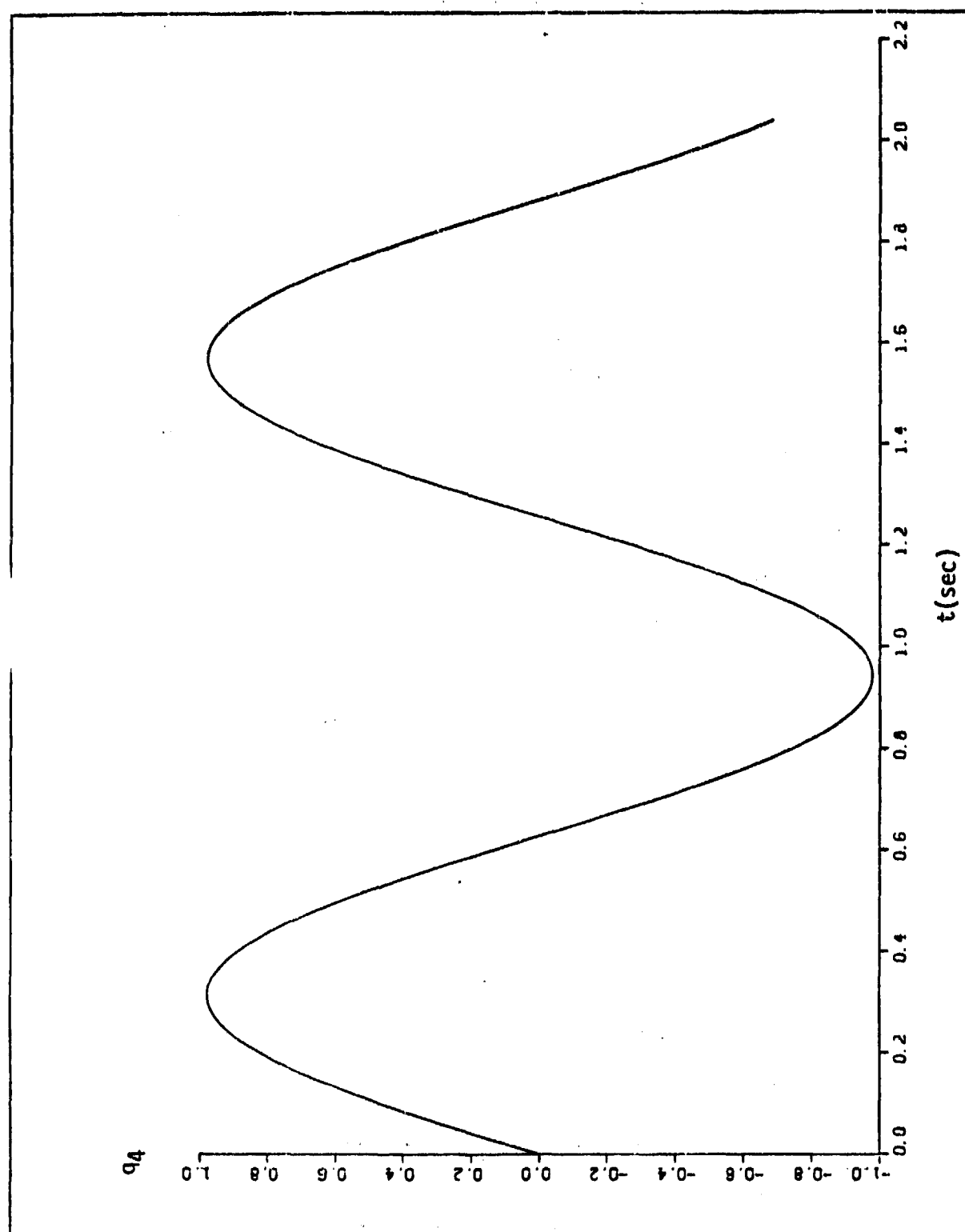


Figure 16  $q_4$  Quaternion

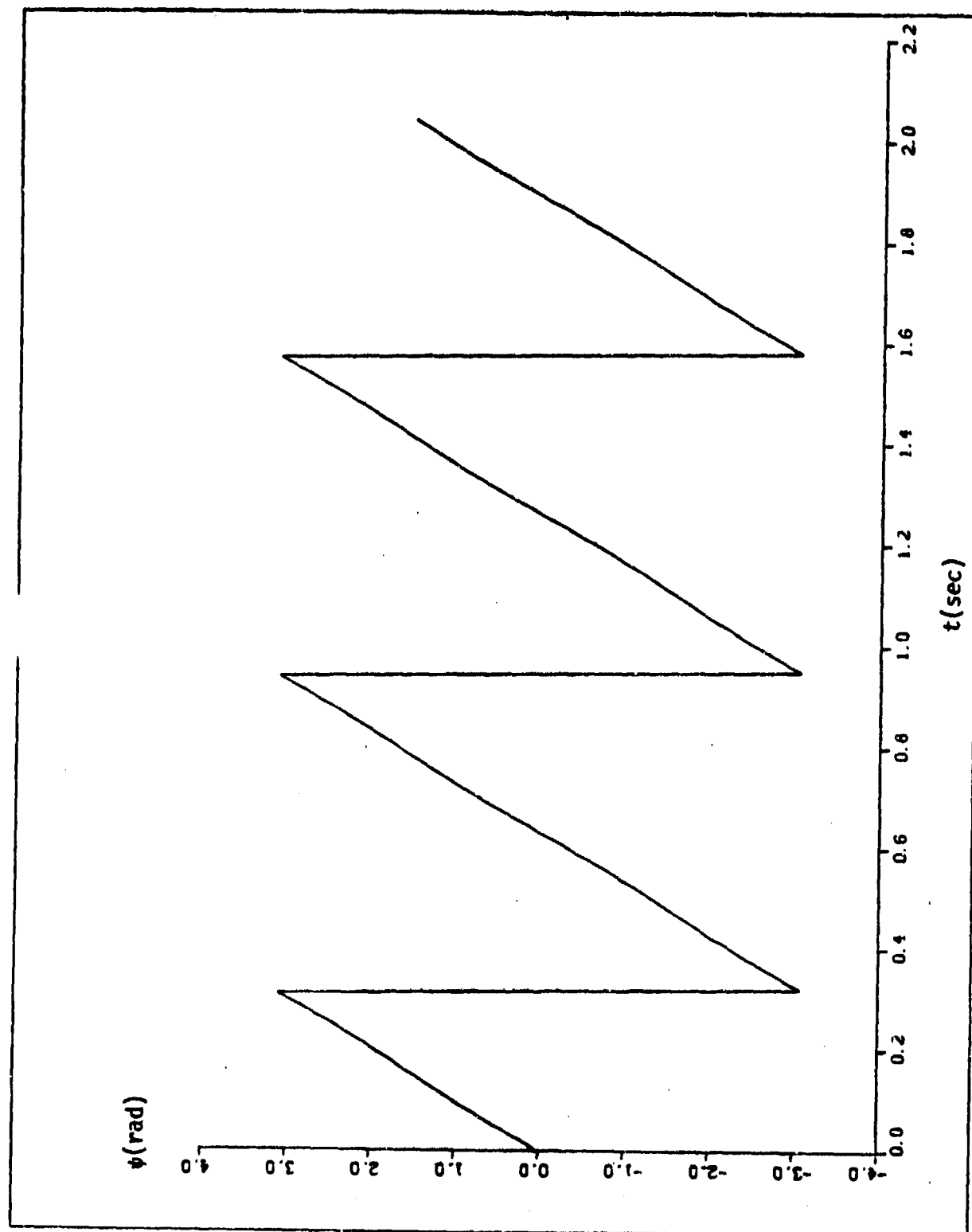


Figure 17 Euler Azimuth Angle

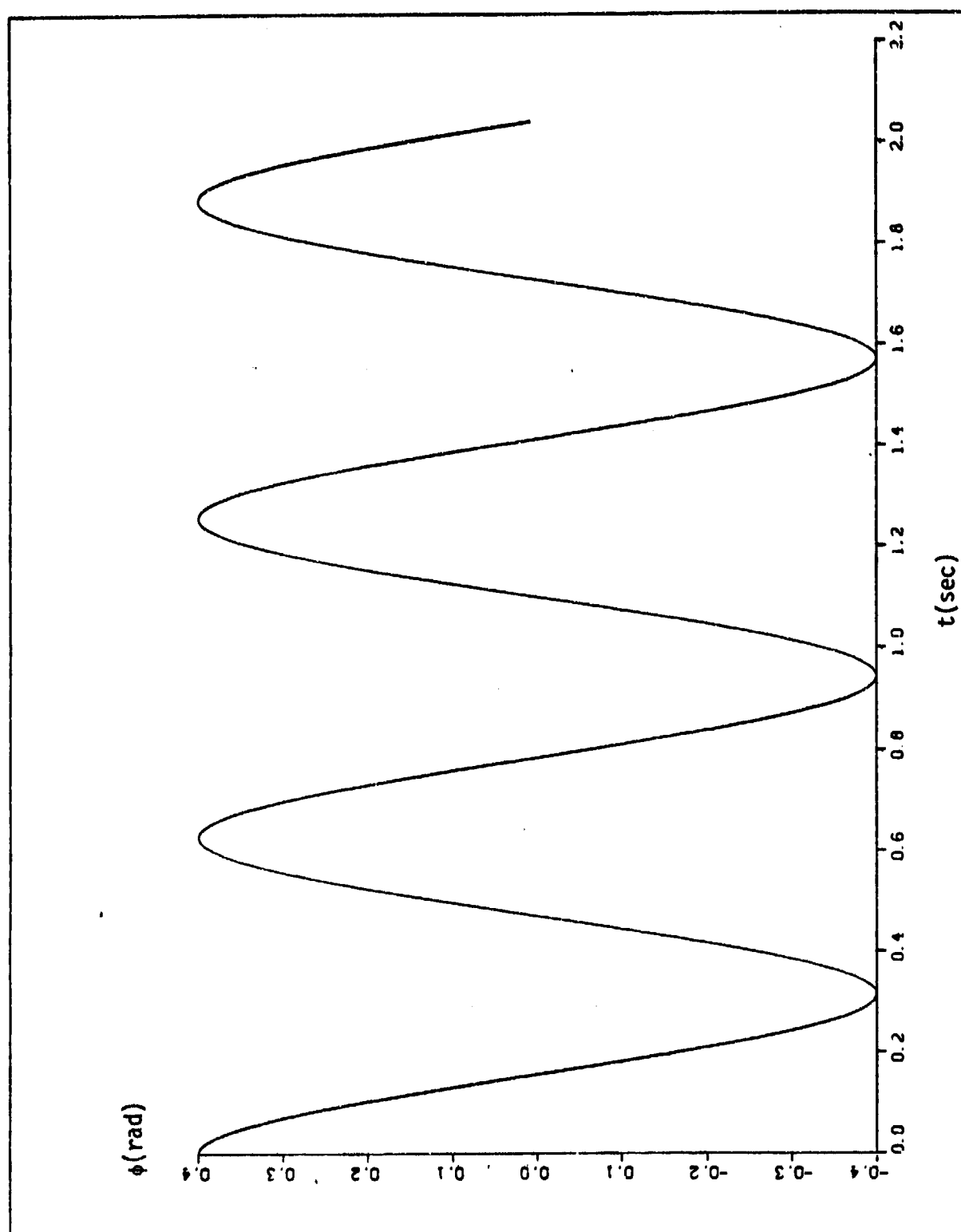


Figure 18 Euler Elevation Angle

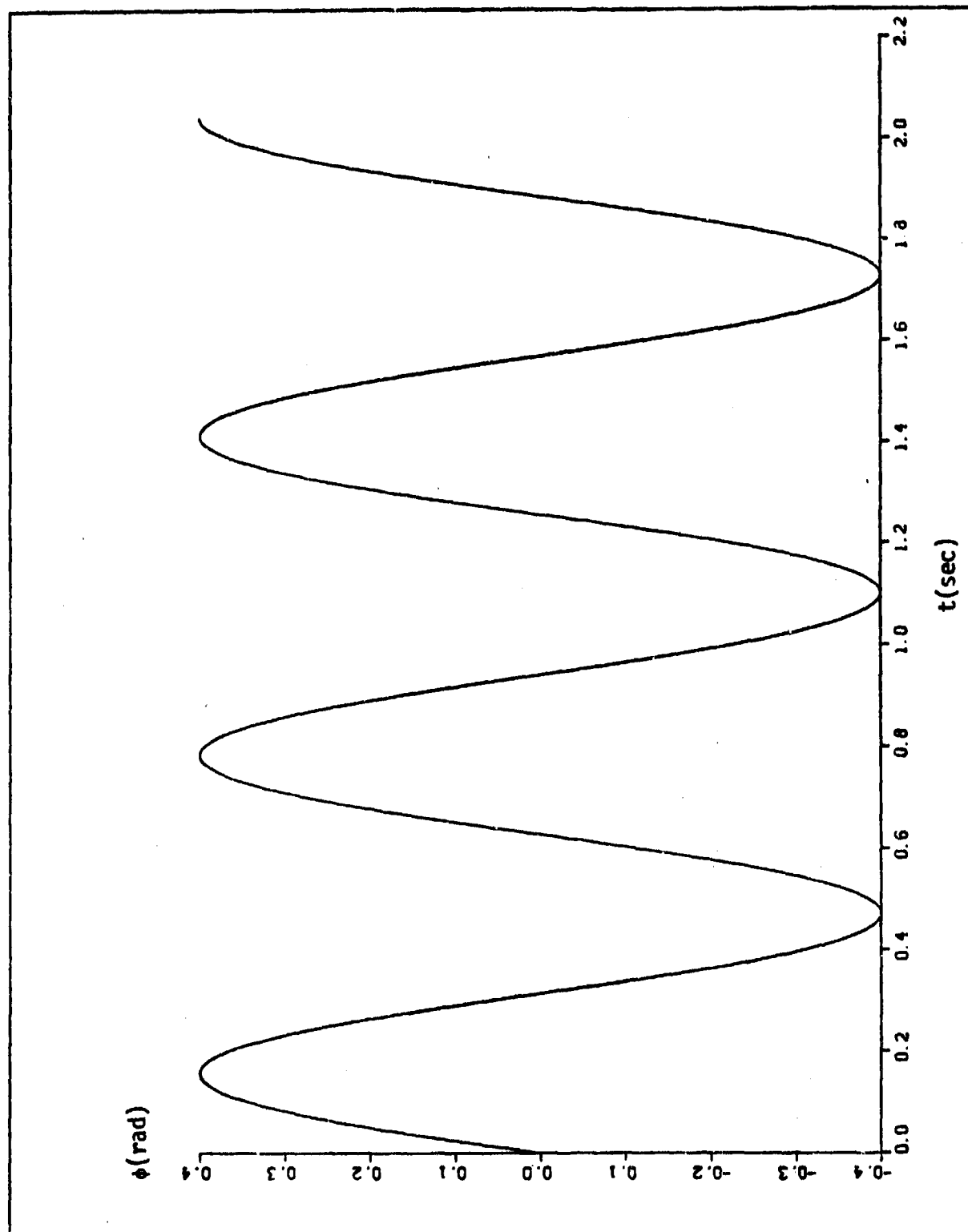


Figure 19 Euler Bank Angle